Kinetic Structure of Low Frequency Continuous Spectrum in General Tokamak Geometry

Yueyan Li[1,2], Matteo Valerio Falessi[2], Philipp Lauber[3], Fulvio Zonca[2,4]

[1] *CREATE Consortium, Via Claudio 21, Napoli, Italy*

[2] *Center for Nonlinear Plasma Science and C.R. ENEA Frascati, C.P. 65, Frascati, Italy*

[3] *MPI für Plasmaphysik, Boltzmannstr. 2, D-85748 Garching, Germany*

[4] *Institute for Fusion Theory and Simulation, Department of Physics, Zhejiang University, Hangzhou, China*

The low frequency kinetic continuous spectra of shear Alfvén waves (SAW) and ion acoustic waves (IAW) in magnetic confinement devices are widely used in identification of frequency gaps and discrete modes. In this work, the numerical model of the drift Alfvén energetic particle stability (DAEPS) code [1] has been extended to include general axisymmetric geometry. The comparison of the numerical code shows that the structure of the low frequency Alfvén continua is sensitive to the shaping effect. The comparison of the kinetic and MHD continuous spectra also suggests that the structure of the kinetic and MHD continua share a similar frequency behavior, while the damping rate of the kinetic continua corresponds to the SAW/IAW coupling. It is also suggested that the ion diamagnetic frequency, corresponding to the plasma nonuniformity, not only changes the frequency, but also destabilizes the KBM/AITG branch near the accumulation point.

I. Drift Alfvén energetic particle stability code

The drift Alfvén energetic particle stability (DAEPS) code [1] is an eigenvalue code using finite element method (FEM) to study low frequency modes excited by energetic particle (EP) in collisionless plasmas, e.g., shear Alfvén wave and drift Alfvén wave physics. The model equations, consisting of quasi-neutrality condition:

$$\left(1+\frac{1}{\tau}\right)\Phi_{\mathrm{P}} = \sum_s \frac{T_i}{e_i^2 n_i}\left\langle e_s \delta K_s \right\rangle, \tag{1}$$

and Schrödinger-like form of vorticity equation:

$$\begin{aligned}&\left(\partial_\theta^2 + \frac{\omega\left(\omega-\omega_{*pi}^T\right)}{\omega_A^2} - \frac{\partial_\theta^2 \kappa_\perp}{\kappa_\perp}\right)\Psi + \frac{\mathrm{J}_b^2 B^2}{\kappa_\perp}\mathbf{b}\times\boldsymbol{\kappa}\cdot\nabla_\perp\left(\frac{\mathbf{b}}{B_0}\cdot\nabla\beta\times\nabla_\perp\Psi\right)\\ &= \sum_s \left\langle \frac{4\pi e_s \mathrm{J}_b^2 B^2}{k_\theta^2 c^2}\frac{T_s}{e_s n_s} J_{0s}\frac{\omega\omega_{ds}}{\kappa_\perp}\delta K_s \right\rangle\end{aligned} \tag{2}$$

are derived within the general fishbone-like dispersion relation (GFLDR) theoretical framework [2, 3], where $\Phi_{\mathrm{P}} = \delta\phi - \delta\psi$ corresponds to the parallel electric field, $\Psi = \delta\psi\kappa_{\perp}$ is the Schrödinger-like potential corresponding to the magnetic scalar potential, $\kappa_{\perp} = k_{\perp} / k_{\theta}$, J_{b} denotes the Jacobian of the Boozer coordinate. The mode structure decomposition (MSD) approach and asymptotic matching between the inertial/singular layer and ideal regions are adopted, which gives the DAEPS code the capability of accurately calculating parallel mode structures in the ballooning space, frequency and growth rate, as well as the asymptotic behavior. Due to the deep connection with GFLDR theoretical framework, the DAEPS code is capable of accurately calculate inertial layer contribution, therefore it can not only calculate the unstable mode, but also damping mode, as well as the electromagnetic continuous spectrum.

The DAEPS code, the Boozer coordinate (r, θ_b, ζ_b) is used to express the general tokamak geometry, where r is the label of the flux surface. After performing the operator and function mapping of ballooning representation, the drift frequency, ignoring the parallel perturbed magnetic field δB_{P}, takes the form of:

$$\begin{aligned} i\omega_{ds} &= i\omega_{ds}^{T} \frac{m_s \mathrm{E}}{T_s}\left(2 - \frac{\lambda B}{B_0}\right)\left(\kappa_n + s\theta\kappa_g\right) \\ &= i\omega_{ds}^{T} \frac{m_s \mathrm{E}}{T_s}\left(2 - \frac{\lambda B}{B_0}\right)\mathrm{g} \end{aligned}, \tag{3}$$

where κ_n and κ_g denote the normal and geodesic curvature, respectively. The drift frequency $\omega_{ds}^{T}(r) = \dfrac{k_{\theta} c T_s}{e_s \bar{B} R_0}$, with $\bar{B}(r) = \dfrac{q\psi'_p}{r}$, and the diamagnetic frequencies $\omega_{*\mathrm{p}s}^{T}(r) = \dfrac{k_{\theta} c T_s}{e_s \bar{B} L_{ps}}$, with $L_{ns}(r) = -\partial_r \ln P_s$, which shares a same formulation of the well-known s-α equilibrium model.

II. Model equations of low frequency continuous spectrum

The model equation for the fluid continuous spectrum is based on the ideal MHD equation with perturbed plasma displacement expressed by the stream function $\boldsymbol{\xi}_{\perp} = \dfrac{c}{B_0}\mathbf{b} \times \nabla\Phi_s$.

Considering the plasma compressibility $\delta P_{comp} = -\Gamma P_0 \nabla \cdot \boldsymbol{\xi}$, where the Γ is the ratio of specific heats, the vorticity equation and the perturbed parallel force balance equation in the inertial region take the form of [4]:

$$\left(\partial_{\theta}^{2} - \Re + \frac{\omega^2}{\omega_A^2}\mathrm{r}^4\right)\Phi_s = q^2 \beta \mathrm{s} \delta P, \tag{4}$$

$$\left(\partial_\theta^2+\frac{\omega^2}{\omega_S^2}\mathsf{r}^2\right)\delta P=2\Gamma\frac{\omega^2}{\omega_S^2}\mathsf{s}\Phi_s\ , \tag{5}$$

where $\delta P = iB_0 R_0 \delta P_{comp} / \left(k_\theta c P\right)$ denotes the normalized perturbed pressure, $\omega_S^2 = \Gamma P / \left[n\left(m_i + m_e\right) q^2 R_0^2\right]$ corresponds to the frequency of the sound wave, $\mathsf{r} = B_0 / B$, $\Re = \left|\nabla r\right|^{-1} \partial_\theta^2 \left|\nabla r\right|$, and $\mathsf{s} = \kappa_g / \left|\nabla r\right|$ are functions with geometric effect.

The numerical model for calculating the kinetic low frequency electromagnetic continuous spectrum is constructed with well circulating particle model, and performing the Fourier expansion, where the gyrokinetic equation can be directly solved, the numerical model of the kinetic continuous spectrum, consisting of vorticity equation and the quasi-neutrality condition, can be further simplified as:

$$\begin{aligned}&-\Lambda_n^2\Psi_n-\sum_p \Re_p\Psi_{n-p}+\sum_p\frac{\omega\left(\omega-\omega_{*pi}^T\right)}{\omega_{A0}^2}\mathsf{r}^4{}_p\Psi_{n-p}\\&=\sum_s\frac{\beta_s}{2}\frac{r^2\left(gq+I\right)^2}{q^2R_0^2\left(\psi_p'\right)^2}\sum_\mu\left[\mathsf{r}^2{}_\mu \mathrm{I}_{n-\mu,s}^{(2)}\frac{\omega}{\omega_{ds}^T}\Phi_{n-\mu}+\sum_p \mathrm{I}_{n-\mu,s}^{(4)}\mathsf{r}^2{}_\mu\mathsf{s}_p\Psi_{n-\mu-p}\right]\end{aligned} \tag{6}$$

$$\left(1+\frac{1}{\tau}-\sum_s \mathrm{I}_{\mathrm{n},s}^{(0)}\right)\frac{\omega}{\omega_{ds}^T}\Phi_n=\mathrm{I}_{\mathrm{n},s}^{(2)}\sum_p \mathsf{s}_p\Psi_{n-p} \tag{7}$$

where $\mathrm{I}_{l,s}^{(n)}$ corresponds to the kinetic contribution of the well circulating particles, and $\Lambda_n = \left(\Lambda + n\right)^2$, with $\Lambda = nq - m = k_{\parallel} J_b B$ corresponds to the parallel wave vector, which also denotes to the inertial layer contribution.

III. Numerical results of the low frequency continuous spectrum

The comparison of the fluid low frequency electromagnetic continuous spectrum with n=5 of DAEPS and FALCON [5] is shown in Figure 1(a), where the FALCON uses the original equilibrium geometric tensor, while the DAEPS uses the analytic s-α model, which suggests that the low frequency continuous spectrum is sensitive to realistic magnetic geometry. The comparison of the fluid and kinetic continuous spectrum with numerical equilibrium, shown in Figure 2(b), suggests that the frequency of the kinetic structure of low frequency spectra is consistent with the fluid result due to the small diamagnetic frequency. Figure 2 shows the comparison of the frequency and growth rate of kinetic continuous spectrum calculated by DAEPS and LIGKA [6] for ITER equilibrium. It is suggested that the frequency of TAE, BAE and KBM branches are highly consistent, and the growth/damping are qualitatively consistent, while the frequency of BAAE branch is consistent near the accumulation point.

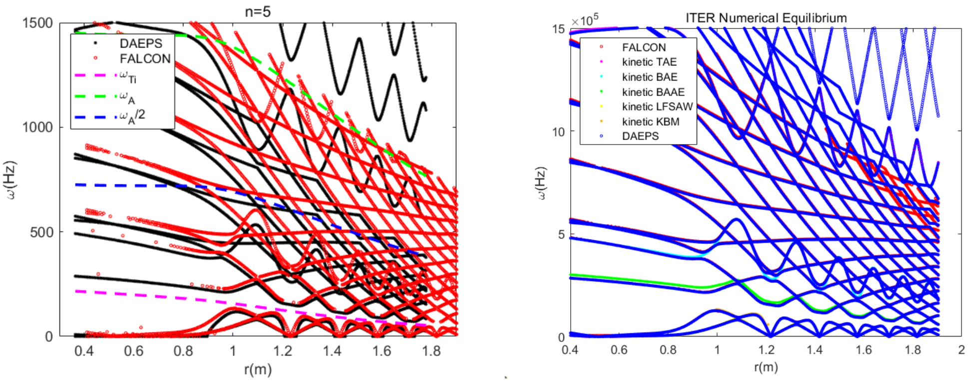

(a) **(b)**

Figure 1. Comparison of the (a) fluid and (b) kinetic low frequency electromagnetic continuous spectrum with n=5 calculated with DAEPs and FALCON.

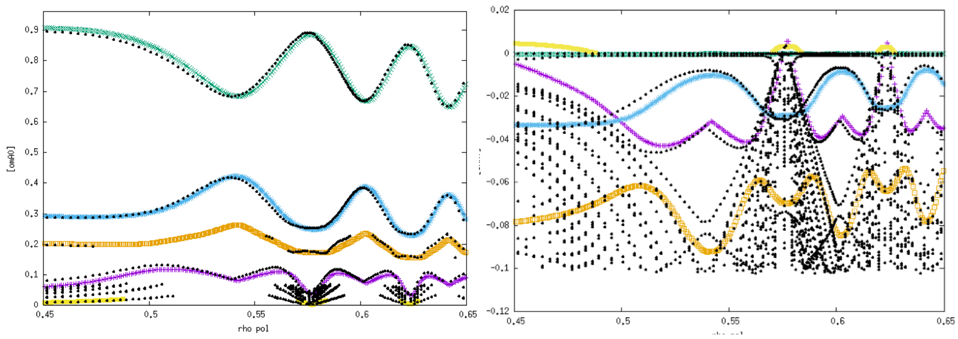

(a) **(b)**

Figure 2. Comparison of the (a) frequency and (a) growth rate of the kinetic low frequency electromagnetic continuous spectrum calculated with DAEPS and LIGKA.

Acknowledgments

This work has been carried out within the framework of the EUROfusion Consortium, funded by the European Union via the Euratom Research and Training Programme (Grant Agreement No 101052200 EUROfusion). Views and opinions expressed are however those of the author(s) only and do not necessarily reflect those of the European Union or the European Commission. Neither the European Union nor the European Commission can be held responsible for them.

References

[1] Li Y, Hu S, Zheng W, Xiao Y. Phys Plasmas. 2020;27(6):062505.

[2] Chen L, Zonca F. Rev Mod Phys. 2016;88(1):015008.

[3] Zonca F, Chen L. Phys Plasmas. 2014;21(7):072120.

[4] Chen L, Zonca F. Phys Plasmas. 2017;24(7):072511.

[5] Falessi MV, Carlevaro N, et al. Phys Plasmas. 2019;26(8).

[6] Lauber P, Günter S, et al. J Comput Phys. 2007;226(1):447-465.